Analyst

The Growing Role of Structural Mass Spectrometry in the Discovery and Development of Therapeutic Antibodies

Journal:	*Analyst*
Manuscript ID	AN-CRV-02-2018-000295.R1
Article Type:	Critical Review
Date Submitted by the Author:	02-Apr-2018
Complete List of Authors:	Tian, Yuwei; University of Michigan, Chemistry Ruotolo, Brandon; University of Michigan, Chemistry

Analyst

Critical Review

The Growing Role of Structural Mass Spectrometry in the Discovery and Development of Therapeutic Antibodies

Received 00th January 20xx,
Accepted 00th January 20xx

DOI: 10.1039/x0xx00000x

www.rsc.org/

Yuwei Tian and Brandon T. Ruotolo*

The comprehensive structural characterization of therapeutic antibodies is of critical importance for the successful discovery and development of such biopharmaceuticals, yet poses many challenges to modern measurement science. Mass spectrometry has evolved into a rapid and sensitive tool for assessing the structures, stabilities, and dynamics of such proteins. Here, we review the current state-of-the-art mass spectrometry technologies focusing on the characterization of antibody-based therapeutics. We conclude by discussing the future of structural mass spectrometry, and its role in enabling the biopharmaceutical pipeline.

Introduction

Over the past few decades, biopharmaceuticals have emerged as an exceptionally important class of therapies, evidenced by the number of approved therapies in this class for indications ranging from cancers to autoimmune diseases.[1] While biopharmaceuticals represent a diverse group of molecular subclasses, monoclonal antibodies (mAbs) and related therapeutics, such as antibody-drug conjugates (ADCs) and bispecific antibodies (bsAbs), are undoubtedly the most promising and fastest growing of these subclasses, owing to their high specificity, high efficacy and fewer side effects.[2–6] As the benefits of biopharmaceuticals are often attributed to their complex molecular compositions and diverse conformations, the challenging task of their comprehensive biophysical characterization is exceptionally important during discovery and development.

Mass spectrometry has emerged to produce a family of methods aimed at addressing the structural complexity of biopharmaceuticals. With concomitant advances in sensitivity, resolution, accuracy, and speed, MS has been widely deployed for the characterization of therapeutic mAbs. In addition to elucidating mAb primary structures, MS methods are capable of probing the higher order structures and dynamics of therapeutic mAbs. In this review, we will focus on recent progress in the development of structural MS tools for the characterization of mAbs and mAb-related therapeutics (Figure 1). Structural MS refers to those MS-based tools focused on the biophysical characterization of protein samples, including the extraction of 3D structure information from MS datasets. In discussing this work, we aim to illustrate the versatility of MS in context of mAb structural characterization. We conclude by discussing the future potential of structural MS in the context of rapidly evolving biopharmaceutical analysis workflows.

Sequencing Intact Antibodies

Department of Chemistry, University of Michigan, Ann Arbor, MI, 48109, USA
Email: bruotolo@umich.edu

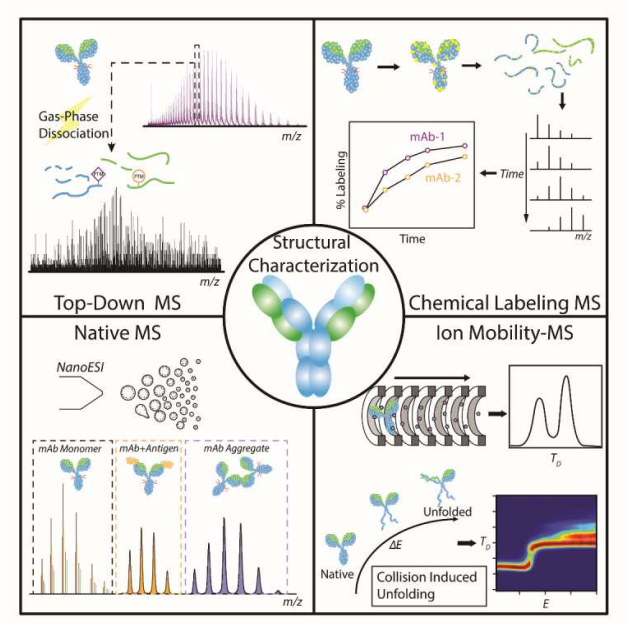

Fig. 1 A schematic diagram illustrating four key structural MS-based technologies used for the characterization of mAbs and mAb-related therapeutics: Top-down MS for sequencing and PTM analysis (*upper-left*), Native MS for assessing intact mass, target binding stoichiometry, and oligomer populations (*bottom-left*), Chemical labeling MS for probing the conformation and dynamics of mAbs (*upper-right*), and ion mobility-MS for characterizing higher order structures and stabilities (*bottom-right*).

Typically, "bottom-up" protein sequencing methods, involving the reduction, alkylation and proteolytic digestion prior to LC/MS/MS, are used to interrogate the primary structures of therapeutic mAbs.[7] Although such strategies are well established, quantifying all the post-translationally modified (PTM) or degraded states for a given mAb can be challenging using such approaches.[8] Top-down mass spectrometry can aid to overcome these challenges by directly introducing intact mAbs into gas phase for PTM assessment and sequencing. Ideally, each mAb isoform is isolated and analyzed individually, for a more comprehensive analysis of mAb PTMs and sequence variants. Despite advances in top-down sequencing technology, complete mAb sequences remain challenging to obtain partially due to the highly structured regions of antibody domains protected by disulfide bonds. As such, middle-down approaches, which involve cleaving mAbs into large peptide fragments via limited enzymatic digestion for tandem MS analysis, are often used to supplement both top-down and bottom-up sequencing data. (Figure. 2) The application of both top-down and middle-down MS workflows toward mAb analysis have been extended through the use of high-resolution MS and a range of ion activation technologies. For example, high resolution Orbitrap and Fourier transform ion cyclotron resonance(FT-ICR) [10,11] are both leveraged in order to reduce mass overlaps within the complex spectra resulting from intact protein fragmentation events. In addition, such platforms are often equipped with a broad range of ion activation technologies, ranging from slow-heating techniques, *e.g.* collision induced dissociation (CID), to rapid ion activation approaches, *e.g.* ultraviolet photodissociation (UVPD), with each providing complementary sets of mAb fragments and enable substantially increased protein sequence coverage values.[12]

Early top-down analyses of mAbs revealed that the variable regions of mAbs can be rapidly characterized by performing in-source CID fragmentation followed by tandem MS, in partnership with accurate time-of-flight (ToF) measurements of the intact mAb.[11] This approach was then further developed by increasing the transmission efficiency for intact mAbs on hybrid linear quadrupole ion trap-Orbitrap (LTQ-Orbitrap) platforms, enabling both intact mass and sequencing data to be acquired on a single platform.[13] Although this approach was able to differentiate IgG2 disulfide isoforms, as well as glutamine and pyro-glutamate variants, the mAb sequence coverage obtained was limited. Workflows incorporating middle-down analyses have achieved greater sequence coverages, permitting the identification of site-specific methionine oxidations[14], as well as detecting drug-product-related impurities and variants[15].

For both top-down and middle-down MS mAb analysis, electron-based ion activation methods have been used to produce extensive sequence-informative fragmentation and breaking disulfide bonds while retaining thermally labile PTMs. For example, online liquid chromatography (LC) has been coupled to electron transfer dissociation (ETD) and high-resolution ToF-MS for the comprehensive top-down structural characterization of two different mAbs.[16] This workflow yielded quantitatively improved sequence coverage when compared to previous protocols, ranging from 15 to 21%, including sequencing information from mAb constant regions that proved transparent to previous CID experiments[13]. Subsequently, a hybrid Orbitrap FTMS workflow incorporating ETD was described and used to sequence samples of

Adalimumab (the biotherapeutic Humira from AbbVie) at LC timescales, achieving ca. 33% sequence coverage.[17] While impressive, this level of sequence coverage has proven challenging to improve upon in recent top-down sequencing experiments, owing primarily to the significant gas-phase stabilities of mAb ions.

In order to further improve mAb sequence data, middle-down ETD-MS data has been integrated with previously described top-down protocols to produce double the sequence coverage compared to previous top-down only analyses. Importantly, the incorporation of middle-down sequencing data has served to unlock sequence information from the entirety of the mAb complementarity determining regions (CDRs), measure mAb glycoforms, and characterize Lys-clipped variants.[18] Another approach to broadening mAb sequence coverage in both top-down and middle-down MS sequencing experiments is to move to alternative ion activation technologies. For example, top-down sequencing of mAbs with electron capture dissociation (ECD) on an FT-ICR MS platform has been shown to provide a greater number of total cleavages than analogous CID or ETD experiments performed on quadrupole (Q)-ToF-MS platforms, and a comparable number of cleavages when compared to ETD sequencing performed using Orbitrap MS.[10] In addition, 193-nm UVPD has been reported to offer detailed sequence analysis for intact mAbs, as well as PTM site localization.[19] The acquisition speed of the UVPD tandem MS experiment makes it an attractive option for performing rapid mAb sequencing experiments on an LC timescale. Further development of hybrid MS ion activation techniques, such as a combination of ETD and higher-energy collision dissociation (EThcD)[20] and ETD combined with UVPD (ETUVPD)[21], promises to further drive the performance of both top-down and middle-down mAb sequence analysis in the future.

Measuring the Stoichiometries of Antibody-associated Complexes

The introduction of soft ionization sources, such as matrix-assisted laser desorption ionization (MALDI)[22] and electrospray ionization (ESI)[23], over thirty years ago enabled the transfer of large biomolecules to gas phase in their intact form, and have significantly strengthened various MS methods used to study biological molecules.[24,25] While the vast majority of mAb sequencing experiments use ions produced under denaturing conditions in order to improve sequence coverage, native MS experiments seek to make mass measurements of mAbs while preserving their structure under native conditions.[26] The vast majority of all native MS experiments utilize ESI-based approaches to form ions directly from native-like solutions, where pH and ionic strength can be easily controlled to produce conditions that preserve mAb structure and function.[27]To enhance the intensities of mAb signals in native MS experiments, Nano-ESI (nESI), utilizing a miniaturized ESI emitter and nL/min flow rates is often used in order to reduce ESI droplet sizes, increase overall ionization efficiency, and increase the overall tolerance of the ion source for salts and other common biotherapeutic excipients.[28] Ammonium

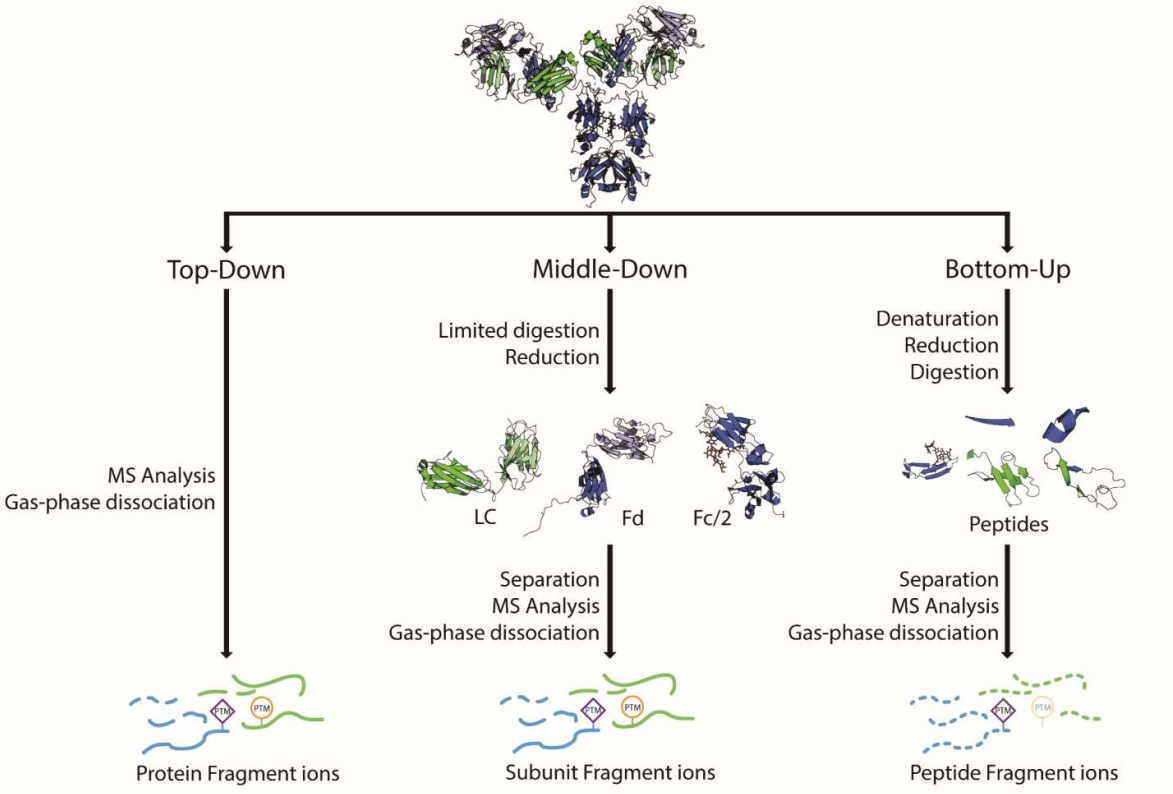

Fig. 2 A schematic diagram comparing Top-Down (*Left*) and Middle-Down (*middle*) MS workflows with Bottom-Up MS protocols (*Right*) for mAb sequencing. For bottom-up MS approaches, proteins are digested into small peptides for LC separation and MS analysis, where peptides are selected and sequenced. Some labile PTMs may be lost during bottom-up workflows. In top-down MS, all proteoforms are directly sequenced in the gas-phase using advanced MS/MS strategies. For middle-down workflows, MS/MS analysis is performed on large fragments or mAb subunits after limited proteolysis in order to maximize both sequence coverage and PTM retention. (LC – light chain; Fd – heavy chain fragment generated from reduction of the antigen binding fragment; Fc/2 – heavy chain fragment obtained after reducing the Fc fragment.)

acetate salts are often used to establish the ionic strength for samples to be analyzed by native MS due to their general volatility. Owing to their folded conformations, fewer total charges are deposited on the mAb, resulting in a narrower charge envelope shifted towards greater mass-to-charge (m/z) values when compared to MS data often acquired under denaturing conditions as part of top-down sequencing experiments. Thus, the equipment used for native MS experiments are typically modified in order to maximize the transmission of high m/z ions. Owing to their wide available mass ranges, modified Q-ToF instruments have been the dominant platform for native MS.[29,30] More recently, Orbitrap and FT-ICR mass analyzers have been described for robust native MS experiments, offering higher resolving power than typical Q-ToF measurments.[31–34]

In the context of mAb analysis, native MS provides accurate intact masses as well as information on glycoform heterogeneity, antibody-antigen binding, and any oligomeric states present.[35–38] For example, native MS data acquired using a modified Orbitrap platform has been used to assign and quantify the heterogeneous glycoforms within a mAb sample.[36] In these spectra, a mass resolving power of up to 12000 at an m/z of 6000 could be achieved, allowing for the confident assignment of antibody glycoforms. In addition to the identification of PTM states, high-resolving power native MS has also been demonstrated to both qualitatively and quantitatively characterize antibody mixutres.[39,40] For example, Q-ToF based native MS has been used to resolve and quantify nine out of ten antibodies present within a mixture, whereas such a mixture could not be similarly unraveled by cation exchange chromatography.[39] Furthermore, using high resolving power native MS, a mixture containing fifteen different antibodies, with mass differences ranging from 20.94 to 1149.41 Da were baseline resolved.[40] Triplicate native MS measurements showed excellent quantitative reproducibility, exhibiting less than 1.2% relative error in the ion intensity values recorded for the resolved mAbs.

The ability to preserve noncovalent protein-protein interactions during the ESI process in native MS workflows enables the direct measurement of antibody-antigen binding stoichiometries and stabilities. Pioneering work in this area[38] demonstrated that complexes formed between the recombinant V antigen (rV), a 37-kDa protein secreted by *Y. pestis,* and its complimentary mAb could be readily detected and characterized. These native MS measurements revealed that the rV antigen forms a tightly associated dimer at micromolar concentrations, that a 1:2 binding stoichiometry is prevalent for the antibody:antigen complex, and quantified the resulting antibody-antigen binding specificity. Later work used native MS to investigate the immune complex formed between the recombinant JAM-A protein, as well as an antigenic protein (Ag) overexpressed in tumor cells, with both murine and humanized mAbs.[41] These data were used to determine both the mAb:antigen binding stoichiometry and selectivity, revealing similar values for both humanized and murine mAbs. As above, the advent of higher resolving power native MS platforms has also been leveraged for the analysis of antibody-antigen complexes.[36] Native MS is also a useful tool for characterizing antibody aggregates, which are common degradation products for therapeutic proteins, causing activity loss, decreased solubility, and enhanced unwanted immunogenicity. Because aggregation can occur during production, formulation and storage, it is critical to monitor aggregate formation through multiple stages of biopharmaceutical development. To this end, the chromatographic separation of protein oligomers was integrated with native MS in order to successfully detect soluble mAb oligomers induced by pH-stress.[35] In addition, native MS has been used to analyze the antigen binding stoichiometry of a functional IgG hexamer.[42] The resulting large multi-protein complex was further characterized by tandem MS, which provided critical information on the spatial arrangement and stoichiometry of the subunits within the assembly.

Antibody related drug products, such as bsAbs and ADCs, have also recently been characterized by native MS workflows. For instance, native MS was used to monitor Fab-arm exchange, a physiological process in which portions of two IgG4 mAbs recombine to form a chimeric bsAbs.[43] Fab-arm exchange was mimicked *in vitro* through the addition of a mild reducing agent, and the dissociation kinetics of IgG4 were monitored by native MS. The results highlighted the importance of the C_H3 domain in the process that gives rise to the ultimate chimeric bsAbs. Native MS was also used to characterize cysteine-linked ADCs, yielding average drug-to-antibody ratio (DAR) values comparable to more time consuming hydrophobic interaction chromatography (HIC) analyses.[44,45] Recent work has also demonstrated the benefits of native MS for characterizing highly heterogeneous lysine-linked ADCs.[46,47] Average DAR values can be accurately deduced from native MS spectra collected for deglycoslyated lysine-linked ADC samples using high resolving power native MS. Furthermore, charge reduction approaches coupled to native MS analysis of ADCs has been used to reduce spectral complexity and decrease mass overlaps for the broadband measurement of highly accurate DAR values.[46]

Probing the Higher Order Structures of Therapeutic Antibodies

A detailed understanding of higher order structure is critically important for developing protein therapeutics. For example, mAb misfolding can lead to a loss of antigen binding affinity, as well as altered aggregation and degradation pathways, all combining to give rise to reduced mAb efficacy and increased immunogenicity.[48,49] Hydrogen/deuterium exchange (HDX) coupled to MS has been used for over twenty-five years to study the dynamics of proteins in solution,[50–52] and is now increasingly applied to mAb analysis. Modern HDX-MS experiments can quantify the flexibility and stability of mAbs at the intact protein, peptide, and amino acid-level (Figure. 3). HDX-MS workflows are typically initiated through the exchange of labile backbone amide hydrogens by diluting

protein samples into a D_2O-containing buffer, which is quenched by lowering the pH after a fixed amount of exchange time. The amount of deuterium uptake can be assessed by both top-down and bottom-up workflows, utilizing rapid activation tools in MS/MS mode experiments to assess exchange levels for individual residues within the protein, while the latter approach is currently more commonly deployed. As the HDX rate is related to protein folding structure and dynamics, differences in deuterium uptake level can be mapped on to protein structures to identify epitopes in antigen-antibody interactions, as well as examine local conformational changes of mAbs provoked by

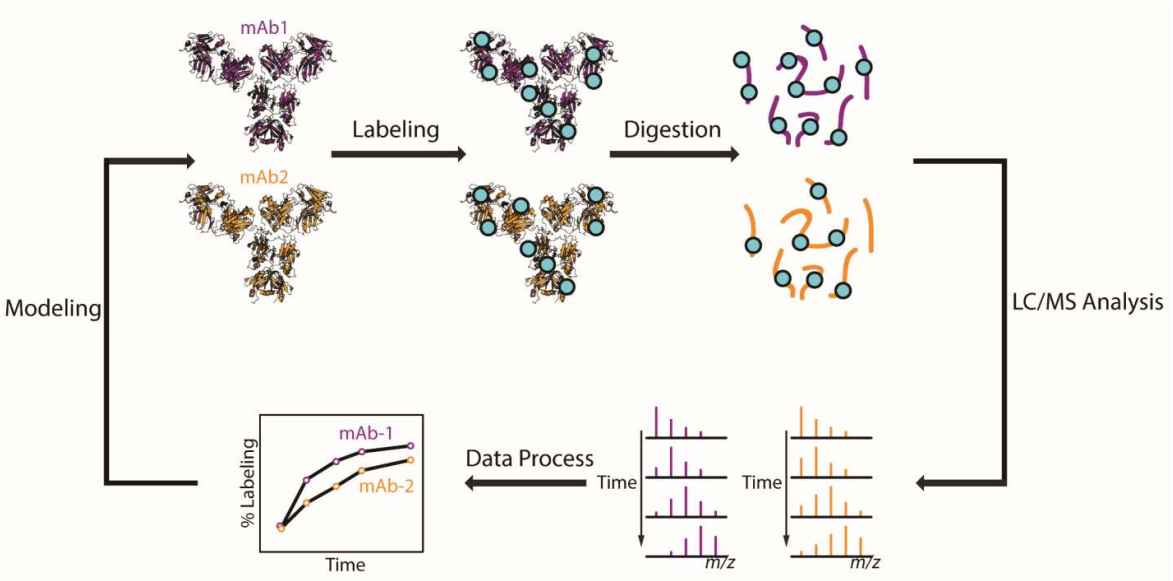

Fig. 3 A generalized workflow for chemical labeling-based structural MS experiments. In the workflow shown, two antibodies are exposed to a chemical label before quenching the labeling reactions. The labeled antibody is then subjected to proteolytic digestion, followed by MS analysis. The mass of each peptide is tracked at each time point and presented as kinetic plot. The data are processed to compare different mAb samples and search of variations in mAb structure and flexibility. If the mAb structure is known, or if a structural model is available, molecular modeling can be performed in order to map conformational differences.

modifications.[53,54]

HDX-MS can be employed to assess mAb conformation and dynamics upon chemical modification, offering benefits to both therapeutic design and quality control protocols. For example, HDX-MS has been used to assess both the global and local conformational dynamics of an IgG1 antibody.[55] Changes in mAb conformation related to deglycosylation were examined using differential HDX-MS analysis, revealing two regions within IgG1 that possess altered protection and were rationalized as critical to FcγRIII receptor binding. The conformational effects of other PTMs, such as galactosylation, fucosylation, methionine oxidation, aspartic acid isomerization, and asparagine deamidation have also been investigated by HDX-MS.[56,57] In particular, HDX-MS has revealed that the complete galactosylation in IgG1, where all mAb glycoforms contain a terminal galactose, results in an increase in structural rigidity within the C_H2 domains in a manner correlated with Fc receptor binding affinity. In contrast, this same study demonstrated that the removal of fucose from the native population of antibody glycoforms did not lead to detectable changes in mAb conformation.

ADCs have also been broadly characterized by HDX-MS, where comparative data can uncover alterations in mAb dynamics perpetrated by both inter-chain disulfide reduction and the presence of conjugated drug molecules.[58] HDX-MS has also been used to assess antibody aggregates, aimed at understanding operative mechanism of mAb self-association.[59–61] For example, HDX-MS analysis of Bevacizumab aggregates induced from multiple freeze/thaw cycles were observed to possess exchange profiles indistinguishable from native mAbs, whereas a similar analysis of thermally-induced aggregates revealed large changes in exchange behavior within mAb CDR regions.[59] Distinct mechanisms for the above stress-induced aggregation events can be extracted directly from the collected data, further highlighting the capabilities of comparative HDX-MS analysis. More recently, the combination of HDX-MS and a spatial aggregation propensity (SAP) algorithm allows identification of aelf-association hotspots in a mAb CDR region, underlining the potential of HDX-MS analysis to direct engineering of therapeutic antibodies in discovery and early development stage.[61] Furthermore, newly developed HDX-MS strategies along with the traditional method have been shown to provide useful insights into the formulation development of mAbs.[62–64]

A separate chemical reactivity-based approach for monitoring protein structure utilizes oxidation chemistry to label protein side chains in a manner correlated with their solvent accessibility. Typically in such oxidative footprinting experiments, susceptible amino acid side chains are irreversibly labeled through hydroxyl radical mediated oxidation at submillisecond time scales. The products of this

oxidation chemistry are then recorded by MS, providing information complementary to HDX-MS experiments.[65] While the details concerning available experimental workflows and general applications of oxidative labeling techniques have been covered by recent reviews,[66–68] here we focus on the uses of this technology for therapeutic mAb analysis. In a manner similar to HDX, the fast photochemical oxidation of proteins (FPOP) has also been used to assess mAb higher order structures and map antibody epitopes. For example, recent work describes the utilization of FPOP for characterizing IgG2 disulfide variants, in which such data identified local conformational changes in the mAb hinge regions, as well as detecting altered protein dynamics within the CDRs for IgG2 mutants in comparison with wild type.[69] This study featured the integration of multiple complementary MS-based methods in order to rapidly characterize antibody mutants. Specifically, FPOP data was supported by both top-down and ion mobility-mass spectrometry (IM-MS) analyses in order to provide a comprehensive view of both mAb conformation and composition. In addition, FPOP has been used to determine the specific residues involved in the epitopes for an anti-interleukin-23 (anti-IL-23) antibody.[70] Although oxidative labeling techniques have not been as widely used in biopharmaceutical industry as HDX due to ongoing challenges associated with automated sample preparation and data processing, it is clear that continuing efforts will integrate this family of tools into the ever evolving roadmap for biopharmaceutical discovery and development.

Simultaneously Assessing the Size, Shape and Stability of Intact Antibodies

Ion mobility (IM) can rapidly separate ions based on their charges and shapes in gas phase under the influence of a weak electric field.[71,72] IM separation can be performed on a wide range of platforms combined with MS detection, such as the drift tubes (DTs) [73,74] and travelling wave ion mobility (TWIM) separators [75–77]. In a typical IM experiment, packets of ions are introduced into an ion guide pressurized with inert neutral gas under the influence of a relatively weak electric field. The larger, more-elongated ions collide more frequently with these gas molecules, and thus take a longer time to traverse the IM separator when compared to smaller and more-compact ions. The output of IM separations is the orientationally-averaged ion-neutral collision cross sections (CCS) for the ions analyzed, and this information can be readily extracted either directly from ion arrival times, or through careful calibration with ions of known CCS.[78] Furthermore, theoretical CCSs can be computed from protein structure models, as well as used as constraints for molecular dynamics simulations, enabling the detailed assessment of protein structural states in the gas phase.[79–81] IM-MS has been employed for the structural analysis of proteins and protein complexes, the separation of small molecule pharmaceutical compounds, the resolution of isomeric metabolites, the deconvolution of complex polymer MS spectra, the identification of carbohydrate structures, and the interrogation of multi-protein complex topology.[82–86] Furthermore, once isolated in the gas phase, ions can be collisionally heated and unfolded in an effort to both record protein stabilities and use gas-phase unfolding patterns as a means of differentiating iso-CCS ions.[87,88] Such collision-induced unfolding (CIU) methods are often used in partnership with IM-MS data in order to study protein higher order structures.

While IM is just beginning to be used to analyze mAb structure and stability, a number of reports showcased the ability of IM-MS to separate structural isoforms of antibody-based therapeutics. For example, early results in this area illustrated that IM can rapidly differentiate IgG2 disulfide-

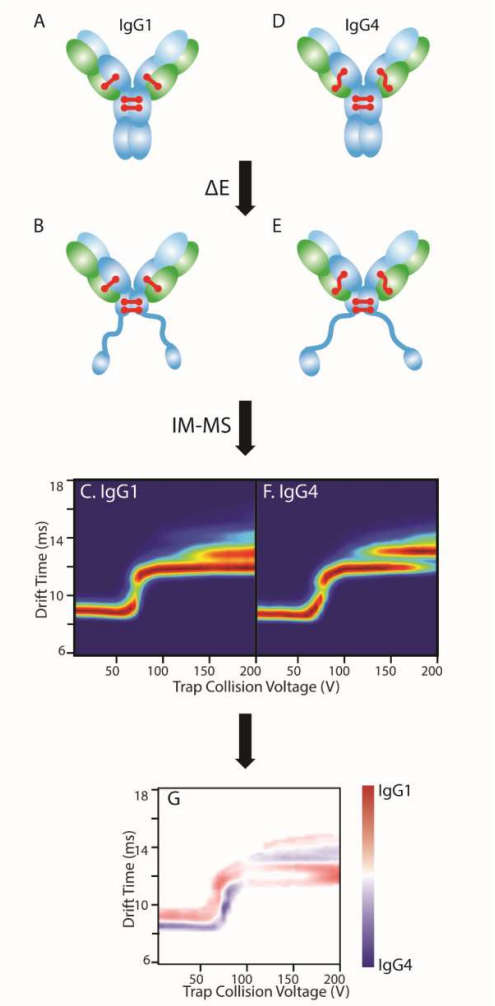

Fig. 4 An example of collision-induced unfolding (CIU) analysis for IgG isoforms. Intact IgG1 (A) and IgG4 (D) are collisionally heated and undergo unfolding (B, E) in the gas phase prior to IM measurement. The IM data are then extracted in order to generate a plot of IM drift time against collision voltage projected as a contour plot (C, F). Once complied, this CIU fingerprint data are compared in order to detect differences in mAb (G). Figure C and F are adapted with permission from Reference 97. Copyright @2015 American Chemical Society.

bonding structure based isoforms.[89] IM-MS data has also shown that intact mAbs are more conformationally diverse than proteins or protein complexes of comparable sizes, as

represented by the peak widths achieved during IM separation.[90] This work, as well as a later report combining CCS data from both DT, TWIM devices with molecular dynamics simulations strongly indicates that mAb ions undergo significant compaction in the gas phase, centering on the hinge region of the mAb structure.[91] In recent work, a combination of IM-MS and HDX-MS was used to probe the global and local dynamics of a series of IgG1 Fc variants.[92] While IM data were nearly identical for lower charge states of three IgG1 Fc variants were, significant differences were observed in the IM data acquired for higher charge states. Overall, the IM-MS data indicated that the IgG1 Fc mutants were more susceptible to gas-phase unfolding when compared to wild type mAbs, consistent with their stabilities in solution. IM-MS data for intact therapeutic antibodies have also been used to rapidly assess the similarity of innovator mAbs and their biosimilars.[93]

In general, antibody isoforms that exhibit CCS differences of greater than 3% can be routinely resolved by IM separation.[77,78,94,95] In many cases, however, local conformational changes caused by PTMs or mutations can be too subtle to be captured by IM separation alone. In such cases, CIU can be used to rapidly resolve such conformational states through differences in their unfolding patterns and stabilities in the gas phase. CIU data is frequently displayed as a 'fingerprint', where the IM drift times or CCS values are plotted against the collision voltages used to heat ions and generate protein unfolding.(Figure 4) Such experiments have been used for a broad array of applications, and the general utility of CIU in the context of small molecule drug discovery and development has been previously reviewed.[96–101] Relatively recently, CIU data has been shown to quantitatively discriminate between IgG subtypes that differ only in terms of their disulfide bonding.[102] For example, IgG1 and IgG4 possess the same number of inter-chain disulfide bonds, and only differ in the disulfide connectivity pattern between their heavy and light chains. In both cases, three main features were observed during CIU. However, detailed comparisons enabled by CIUSuite software[103] revealed clear differences within the CIU datasets. Continuing work in this area has seen CIU used to differentiate innovator and biosimilar preparations of infliximab, in which minor differences in mAb glycosylation and glycation across multiple sample lots produced measurable shifts in mAb unfolding.[104] More recently, the combination of native IM-MS and CIU distinguished complexes formed between a single antigen and various antibodies binding to different epitopes.[105]

In addition to coupling with native MS for intact protein analysis, IM-MS has also been used extensively to separate and analyze complex peptide carbohydrate mixtures. The potential of IM-MS to distinguish lot-to-lot variability within mAb N-glycosylation profiles was recently reported.[106] Although such techniques have not been applied to therapeutic proteins yet, the utility of IM-MS for in-depth structural analysis of carbohydrate and glycoconjugate has been illustrated generally, thus illuminate the clear benefits that such workflows will provide for the characterization of therapeutic antibodies [107–109]

Conclusions and Outlook

Structural mass spectrometry offers a variety of approaches for the in-depth characterization of therapeutic antibodies. Such technologies can probe all levels of mAb structure, including their primary structures and PTMs, enabling the detailed assessment of mAb variants within complex mixtures. Higher-order structure data can be extracted directly from MS-based technologies as well, enabling the stoichiometry of antibody-antigen complexes, mAb stability, dynamics, and overall size to be assessed rapidly from relatively impure samples.

There are many challenges associated with the further development of structural MS techniques for mAb analysis. Clearly, therapeutic proteins equally modified on different sites are exceptionally challenging to separate by MS alone, greatly complicating their differential analysis. Furthermore, the data interpretation steps for many structural MS techniques continues to be a bottle-neck generally, but also specifically in the context of mAb analyses. In addition, automated sample handling and high-throughput sample delivery systems have yet to be completely integrated with structural MS workflows. Despite the clear synergy of structural MS-based approaches, integration of these data types has remained challenging. Clearly, the facile integration of such data would enable generating high-quality structural models for large biopharmaceuticals that resist characterization by NMR or X-ray crystallography. Overall, we expect that continued developments in all of these areas will further drive our ability to discover and develop the next generation of therapeutic antibodies, as well as substantially improve our ability to assess biosimilars, thus enabling the continued growth of this exciting class of therapeutics and their profound impact on human health.

Conflicts of Interest

There are no conflicts of interest to declare.

Acknowledgement

Work in Ruotolo lab aimed at developing ion mobility-mass spectrometry and collision induced unfolding methods applied to biopharmaceutical characterization is supported by the National Science Foundation (CAREER 1253384).

References

1 G. Walsh, *Nat. Biotechnol.*, 2014, **32**, 992–1000.
2 J. M. Reichert, *MAbs*, 2012, **4**, 413–415.
3 D. M. Ecker, S. D. Jones and H. L. Levine, *MAbs*, 2015, **7**, 9–14.
4 A. M. Scott, J. D. Wolchok and L. J. Old, *Nat. Rev.*, 2012, **12**, 278–287.
5 R. V. J. Chari, M. L. Miller and W. C. Widdison, *Angew. Chem. Int. Ed. Engl.*, 2014, **53**, 3796–827.
6 J. M. Reichert, *MAbs*, 2017, **9**, 167–181.

7 D. Ren, G. D. Pipes, D. Liu, L. Y. Shih, A. C. Nichols, M. J. Treuheit, D. N. Brems and P. V. Bondarenko, *Anal. Biochem.*, 2009, **392**, 12–21.
8 S. Fodor and Z. Zhang, *Anal. Biochem.*, 2006, **356**, 282–290.
9 A. D. Catherman, O. S. Skinner, N. L. Kelleher, F. Badalà, K. Nouri-mahdavi and D. A. Raoof, *Biochem. Biophys. Res. Commun.*, 2014, **445**, 683–693.
10 Y. Mao, S. G. Valeja, J. C. Rouse, C. L. Hendrickson and A. G. Marshall, *Anal. Chem.*, 2013, **85**, 4239–4246.
11 Z. Zhang and B. Shah, *Anal. Chem.*, 2007, **79**, 5723–5729.
12 J. S. Brodbelt, *Anal. Chem.*, 2016, **88**, 30–51.
13 P. V. Bondarenko, T. P. Second, V. Zabrouskov, A. A. Makarov and Z. Zhang, *J. Am. Soc. Mass Spectrom.*, 2009, **20**, 1415–1424.
14 J. Zhang, H. Liu and V. Katta, *J. Mass Spectrom.*, 2010, **45**, 112–20.
15 D. Wang, C. Wynne, F. Gu, C. Becker, J. Zhao, H. M. Mueller, H. Li, M. Shameem and Y. H. Liu, *Anal. Chem.*, 2015, **87**, 914–921.
16 Y. O. Tsybin, L. Fornelli, C. Stoermer, M. Luebeck, J. Parra, S. Nallet, F. M. Wurm and R. Hartmer, *Anal. Chem.*, 2011, **83**, 8919–8927.
17 L. Fornelli, E. Damoc, P. M. Thomas, N. L. Kelleher, K. Aizikov, E. Denisov, A. Makarov and Y. O. Tsybin, *Mol. Cell. Proteomics*, 2012, **11**, 1758–67.
18 L. Fornelli, D. Ayoub, K. Aizikov, A. Beck and Y. O. Tsybin, *Anal. Chem.*, 2014, **86**, 3005–12.
19 V. C. Cotham and J. S. Brodbelt, *Anal. Chem.*, 2016, **88**, 4004–4013.
20 L. Fornelli, D. Ayoub, K. Aizikov, X. Liu, E. Damoc, P. A. Pevzner, A. Makarov, A. Beck and Y. O. Tsybin, *J. Proteomics*, 2017, **159**, 67–76.
21 J. R. Cannon, D. D. Holden and J. S. Brodbelt, *Anal. Chem.*, 2014, **86**, 10970–10977.
22 M. Karas, D. Bachmann, U. Bahr and F. Hillenkamp, *Int. J. Mass Spectrom. Ion Process.*, 1987, **78**, 53–68.
23 J. B. Fenn, M. Mann, C. K. Meng, S. F. Wong and C. M. Whitehouse, *Science*, 1989, **246**, 64–71.
24 J. a Loo, *Mass Spectrom. Rev.*, 1997, **16**, 1–23.
25 J. a. Loo, *Int. J. Mass Spectrom.*, 2000, **200**, 175–186.
26 A. J. R. Heck, *Nat. Methods*, 2008, **5**, 927–933.
27 P. Kebarle and U. H. Verkerk, *Mass Spectrom. Rev.*, 2009, **28**, 898–917.
28 A. El-Faramawy, K. W. M. Siu and B. a Thomson, *J. Am. Soc. Mass Spectrom.*, 2005, **16**, 1702–7.
29 F. Sobott, H. Hernández, M. G. McCammon, M. a. Tito and C. V. Robinson, *Anal. Chem.*, 2002, **74**, 1402–1407.
30 R. H. H. Van Den Heuvel, E. Van Duijn, H. Mazon, S. A. Synowsky, K. Lorenzen, C. Versluis, S. J. J. Brouns, D. Langridge, J. Van Der Oost, J. Hoyes and A. J. R. Heck, *Anal. Chem.*, 2006, **78**, 7473–7483.
31 R. J. Rose, E. Damoc, E. Denisov, A. Makarov and A. J. R. Heck, *Nat. Methods*, 2012, **9**, 1084–1086.
32 M. E. Belov, E. Damoc, E. Denisov, P. D. Compton, S. Horning, A. A. Makarov and N. L. Kelleher, *Anal. Chem.*, 2013, **85**, 11163–11173.
33 H. Zhang, W. Cui, J. Wen, R. E. Blankenship and M. L. Gross, *J. Am. Soc. Mass Spectrom.*, 2010, **21**, 1966–1968.
34 H. Zhang, W. Cui, J. Wen, R. E. Blankenship and M. L. Gross, *Anal. Chem.*, 2011, **83**, 5598–5606.
35 B. Kükrer, V. Filipe, E. Van Duijn, P. T. Kasper, R. J. Vreeken, A. J. R. Heck and W. Jiskoot, *Pharm. Res.*, 2010, **27**, 2197–2204.
36 S. Rosati, R. J. Rose, N. J. Thompson, E. Van Duijn, E. Damoc, E. Denisov, A. Makarov and A. J. R. Heck, *Angew. Chemie - Int. Ed.*, 2012, **51**, 12992–12996.
37 N. J. Thompson, S. Rosati and A. J. R. Heck, *Methods*, 2014, **65**, 11–7.
38 M. a Tito, J. Miller, N. Walker, K. F. Griffin, E. D. Williamson, D. Despeyroux-Hill, R. W. Titball and C. V Robinson, *Biophys. J.*, 2001, **81**, 3503–3509.
39 S. Rosati, N. J. Thompson, A. Barendregt, L. J. A. Hendriks, A. B. H. Bakker, J. De Kruif, M. Throsby, E. Van Duijn and A. J. R. Heck, *Anal. Chem.*, 2012, **84**, 7227–7232.
40 N. J. Thompson, L. J. a Hendriks, J. De Kruif, M. Throsby and A. J. R. Heck, *MAbs*, 2014, **6**, 197–203.
41 C. Atmanene, E. Wagner-Rousset, M. Malissard, B. Chol, A. Robert, N. Corvaïa, A. Van Dorsselaer, A. Beck and S. Sanglier-Cianférani, *Anal. Chem.*, 2009, **81**, 6364–6373.
42 A. Dyachenko, G. Wang, M. Belov, A. Makarov, R. N. de Jong, E. T. J. van den Bremer, P. W. H. I. Parren and A. J. R. Heck, *Anal. Chem.*, 2015, **87**, 6095–6102.
43 R. J. Rose, A. F. Labrijn, E. T. J. Van Den Bremer, S. Loverix, I. Lasters, P. H. C. Van Berkel, J. G. J. Van De Winkel, J. Schuurman, P. W. H. I. Parren and A. J. R. Heck, *Structure*, 2011, **19**, 1274–1282.
44 J. Chen, S. Yin, Y. Wu and J. Ouyang, *Anal. Chem.*, 2013, **85**, 1699–704.
45 F. Debaene, A. Bœuf, E. Wagner-Rousset, O. Colas, D. Ayoub, N. Corvaïa, A. Van Dorsselaer, A. Beck and S. Cianférani, *Anal. Chem.*, 2014, **86**, 10674–10683.
46 J. Marcoux, T. Champion, O. Colas, E. Wagner-Rousset, N. Corvaïa, A. Van Dorsselaer, A. Beck and S. Cianférani, *Protein Sci.*, 2015, **24**, 1210–1223.
47 I. D. G. Campuzano, C. Netirojjanakul, M. Nshanian, J. L. Lippens, D. P. A. Kilgour, S. L. Van Orden and J. Loo, *Anal. Chem.*, 2017, acs.analchem.7b03021.
48 A. S. De Groot and D. W. Scott, *Trends Immunol.*, 2007, **28**, 482–490.
49 I. a. Kaltashov, C. E. Bobst, R. R. Abzalimov, G. Wang, B. Baykal and S. Wang, *Biotechnol. Adv.*, 2012, **30**, 210–222.
50 V. Katta, B. T. Chait and S. Carr, *Rapid Commun. Mass Spectrom.*, 1991, **5**, 214–217.
51 G. F. Pirrone, R. E. Iacob and J. R. Engen, *Anal. Chem.*, 2015, **87**, 99–118.
52 J. R. Engen and T. E. Wales, *Annu. Rev. Anal. Chem.*, 2015, **8**, 127–148.
53 H. Wei, J. Mo, L. Tao, R. J. Russell, A. A. Tymiak, G. Chen, R. E. Iacob and J. R. Engen, *Drug Discov. Today*, 2014, **19**, 95–102.
54 D. D. Weis, *Hydrogen Exchange Mass Spectrometry of Proteins*, John Wiley & Sons, Ltd, Chichester, UK, 2016.
55 D. Houde, J. Arndt, W. Domeier, S. Berkowitz and J. R. Engen, *Anal. Chem.*, 2009, **81**, 2644–2651.

56 D. Houde, Y. Peng, S. a Berkowitz and J. R. Engen, *Mol. Cell. Proteomics*, 2010, **9**, 1716–1728.

57 A. Zhang, P. Hu, P. MacGregor, Y. Xue, H. Fan, P. Suchecki, L. Olszewski and A. Liu, *Anal. Chem.*, 2014, **86**, 3468–75.

58 L. Y. Pan, O. Salas-Solano and J. F. Valliere-Douglass, *Anal. Chem.*, 2014, **86**, 2657–64.

59 A. Zhang, S. K. Singh, M. R. Shirts, S. Kumar and E. J. Fernandez, *Pharm. Res.*, 2012, **29**, 236–50.

60 R. E. Iacob, G. M. Bou-Assaf, L. Makowski, J. R. Engen, S. A. Berkowitz and D. Houde, *J. Pharm. Sci.*, 2013, **102**, 4315–4329.

61 C. L. Dobson, P. W. A. Devine, J. J. Phillips, D. R. Higazi, C. Lloyd, B. Popovic, J. Arnold, A. Buchanan, A. Lewis, J. Goodman, C. F. van der Walle, P. Thornton, L. Vinall, D. Lowne, A. Aagaard, L.-L. Olsson, A. Ridderstad Wollberg, F. Welsh, T. K. Karamanos, C. L. Pashley, M. G. Iadanza, N. A. Ranson, A. E. Ashcroft, A. D. Kippen, T. J. Vaughan, S. E. Radford and D. C. Lowe, *Sci. Rep.*, 2016, **6**, 38644.

62 J. Arora, J. M. Hickey, R. Majumdar, R. Esfandiary, S. M. Bishop, H. S. Samra, C. R. Middaugh, D. D. Weis and D. B. Volkin, *MAbs*, 2015, **7**, 525–539.

63 D. Houde, Z. E. Nazari, G. M. Bou-Assaf, A. S. Weiskopf and K. D. Rand, *J. Am. Soc. Mass Spectrom.*, 2016, **27**, 669–676.

64 J. Arora, S. B. Joshi, C. R. Middaugh, D. D. Weis and D. B. Volkin, *J. Pharm. Sci.*, 2017, **106**, 1508–1518.

65 D. M. Hambly and M. L. Gross, *J. Am. Soc. Mass Spectrom.*, 2005, **16**, 2057–2063.

66 G. Xu and M. R. Chance, *Chem. Rev.*, 2007, **107**, 3514–3543.

67 L. Konermann, B. B. Stocks, Y. Pan and X. Tong, *Mass Spectrom. Rev.*, 2009, **47**, n/a-n/a.

68 J. B. Sperry and L. M. Jones, in *Biophysical Methods for Biotherapeutics*, John Wiley & Sons, Inc., Hoboken, NJ, USA, 2014, pp. 151–172.

69 L. M. Jones, H. Zhang, W. Cui, S. Kumar, J. B. Sperry, J. a Carroll and M. L. Gross, *J. Am. Soc. Mass Spectrom.*, 2013, **24**, 835–45.

70 J. Li, H. Wei, S. R. Krystek, D. Bond, T. M. Brender, D. Cohen, J. Feiner, N. Hamacher, J. Harshman, R. Y.-C. Huang, S. H. Julien, Z. Lin, K. Moore, L. Mueller, C. Noriega, P. Sejwal, P. Sheppard, B. Stevens, G. Chen, A. A. Tymiak, M. L. Gross and L. A. Schneeweis, *Anal. Chem.*, 2017, **89**, 2250–2258.

71 E. A. Mason and E. W. McDaniel, *Transport Properties of Ions in Gases*, Wiley-VCH Verlag GmbH & Co. KGaA, Weinheim, FRG, 1988.

72 A. B. Kanu, P. Dwivedi, M. Tam, L. Matz and H. H. Hill, *J. Mass Spectrom.*, 2008, 43, 1–22.

73 T. Wyttenbach and M. Bowers, *Int J Mass Spectrom*, 2011, **212**, 13–23.

74 S. R. Harvey, C. E. MacPhee and P. E. Barran, *Methods*, 2011, **54**, 454–461.

75 S. D. Pringle, K. Giles, J. L. Wildgoose, J. P. Williams, S. E. Slade, K. Thalassinos, R. H. Bateman, M. T. Bowers and J. H. Scrivens, *Int. J. Mass Spectrom.*, 2007, **261**, 1–12.

76 K. Giles, J. P. Williams and I. Campuzano, *Rapid Commun. Mass Spectrom.*, 2011, **25**, 1559–1566.

77 Y. Zhong, S.-J. Hyung and B. T. Ruotolo, *Analyst*, 2011, **136**, 3534–3541.

78 M. F. Bush, Z. Hall, K. Giles, J. Hoyes, C. V. Robinson and B. T. Ruotolo, *Anal. Chem.*, 2010, **82**, 9557–9565.

79 A. A. Shvartsburg and M. F. Jarrold, *Chem. Phys. Lett.*, 1996, **261**, 86–91.

80 M. F. Mesleh, J. M. Hunter, A. A. Shvartsburg, G. C. Schatz and M. F. Jarrold, *J. Phys. Chem.*, 1996, **100**, 16082–16086.

81 J. L. P. Benesch and B. T. Ruotolo, *Curr. Opin. Struct. Biol.*, 2011, **21**, 641–649.

82 B. T. Ruotolo, J. L. P. Benesch, A. M. Sandercock, S.-J. Hyung and C. V Robinson, *Nat. Protoc.*, 2008, **3**, 1139–52.

83 J. M. Koomen, B. T. Ruotolo, K. J. Gillig, J. A. McLean, D. H. Russell, M. Kang, K. R. Dunbar, K. Fuhrer, M. Gonin and J. A. Schultz, *Anal. Bioanal. Chem.*, 2002, **373**, 612–617.

84 A. Arcella, G. Portella, M. L. Ruiz, R. Eritja, M. Vilaseca, V. Gabelica and M. Orozco, *J. Am. Chem. Soc.*, 2012, **134**, 6596–6606.

85 H. Li, B. Bendiak, W. F. Siems, D. R. Gang and H. H. Hill, *Anal. Chem.*, 2013, **85**, 2760–2769.

86 F. Lanucara, S. W. Holman, C. J. Gray and C. E. Eyers, *Nat. Chem.*, 2014, **6**, 281–94.

87 K. B. Shelimov and M. F. Jarrold, *J. Am. Chem. Soc.*, 1997, **119**, 2987–2994.

88 S.-J. Hyung, C. V Robinson and B. T. Ruotolo, *Chem. Biol.*, 2009, **16**, 382–90.

89 D. Bagal, J. F. Valliere-Douglass, A. Balland and P. D. Schnier, *Anal. Chem.*, 2010, **82**, 6751–5.

90 K. J. Pacholarz, M. Porrini, R. a Garlish, R. J. Burnley, R. J. Taylor, A. J. Henry and P. E. Barran, *Angew. Chem. Int. Ed. Engl.*, 2014, **53**, 7765–9.

91 I. D. G. Campuzano, C. Larriba, D. Bagal and P. D. Schnier, in *ACS Symposium Series*, 2015, vol. 1202, pp. 75–112.

92 M. J. Edgeworth, J. J. Phillips, D. C. Lowe, A. D. Kippen, D. R. Higazi and J. H. Scrivens, *Angew. Chemie Int. Ed.*, 2015, **54**, 15156–15159.

93 A. Beck, F. Debaene, H. Diemer, E. Wagner-Rousset, O. Colas, A. Van Dorsselaer and S. Cianférani, *J. Mass Spectrom.*, 2015, **50**, 285–297.

94 M. F. Bush, I. D. G. Campuzano and C. V. Robinson, *Anal. Chem.*, 2012, **84**, 7124–7130.

95 R. Salbo, M. F. Bush, H. Naver, I. Campuzano, C. V. Robinson, I. Pettersson, T. J. D. Jørgensen and K. F. Haselmann, *Rapid Commun. Mass Spectrom.*, 2012, **26**, 1181–1193.

96 L. Han, S. J. Hyung, J. J. S. Mayers and B. T. Ruotolo, *J. Am. Chem. Soc.*, 2011, **133**, 11358–11367.

97 L. Han, S. J. Hyung and B. T. Ruotolo, *Angew. Chemie - Int. Ed.*, 2012, **51**, 5692–5695.

98 J. N. Rabuck, S. Hyung, K. S. Ko, C. C. Fox, M. B. Soellner and B. T. Ruotolo, *Anal. Chem.*

99 A. Laganowsky, E. Reading, T. M. Allison, M. B. Ulmschneider, M. T. Degiacomi, A. J. Baldwin and C. V Robinson, *Nature*, 2014, **510**, 172–5.

100 Y. Zhong, L. Han and B. T. Ruotolo, *Angew. Chem. Int. Ed. Engl.*, 2014, **53**, 9209–12.

101 S. Niu, J. N. Rabuck and B. T. Ruotolo, *Curr. Opin. Chem.*

Biol., 2013, **17**, 809–17.
102 Y. Tian, L. Han, A. C. Buckner and B. T. Ruotolo, *Anal. Chem.*, 2015, **87**, 11509–11515.
103 J. D. Eschweiler, J. N. Rabuck-Gibbons, Y. Tian and B. T. Ruotolo, *Anal. Chem.*, 2015, **87**, 11516–11522.
104 K. Pisupati, Y. Tian, S. Okbazghi, A. Benet, R. Ackermann, M. Ford, S. Saveliev, C. M. Hosfield, M. Urh, E. Carlson, C. Becker, T. J. Tolbert, S. P. Schwendeman, B. T. Ruotolo and A. Schwendeman, *Anal. Chem.*, 2017, **89**, 4838–4846.
105 Y. Huang, N. D. Salinas, E. Chen, N. H. Tolia and M. L. Gross, *J. Am. Soc. Mass Spectrom.*, 2017, 24–27.
106 C. W. N. Damen, W. Chen, A. B. Chakraborty, M. van Oosterhout, J. R. Mazzeo, J. C. Gebler, J. H. M. Schellens, H. Rosing and J. H. Beijnen, *J. Am. Soc. Mass Spectrom.*, 2009, **20**, 2021–2033.
107 Y. Huang, A. Gelb and E. Dodds, *Curr. Metabolomics*, 2014, **1**, 291–305.
108 P. Both, A. P. Green, C. J. Gray, R. Šardzík, J. Voglmeir, C. Fontana, M. Austeri, M. Rejzek, D. Richardson, R. A. Field, G. Widmalm, S. L. Flitsch and C. E. Eyers, *Nat Chem*, 2014, **6**, 65–74.
109 J. Hofmann, H. S. Hahm, P. H. Seeberger and K. Pagel, *Nature*, 2015, **526**, 241–244.